Available online at www.sciencedirect.com

SCIENCE DIRECT®

Solid State Ionics 176 (2005) 1169–1174

SOLID STATE IONICS

www.elsevier.com/locate/ssi

Manganese oxide/MWNTs composite electrodes for supercapacitors

Gui-Xin Wang*, Bo-Lan Zhang, Zuo-Long Yu*, Mei-Zhen Qu

Chengdu Institute of Organic Chemistry, Chinese Academy of Sciences, No. 9, Block 4, Renmin South Road, Chengdu 610041,
Graduate School of the Chinese Academy of Sciences, China

Received 31 August 2004; received in revised form 2 February 2005; accepted 7 February 2005

Abstract

Manganese oxide/multiwalled carbon nanotubes (MWNTs) composite was prepared by mixing manganese oxide and MWNTs through a means of ultrasonic vibration in ethanol solution. A nonaqueous hybrid supercapacitor using manganese oxide/MWNTs (M/M) composite and MWNTs as positive and negative electrodes, respectively, has been designed and investigated by constant current charge/discharge tests. The asymmetric hybrid capacitor has better capacitance and energy characteristics than those of the symmetric ones based on individual M/M composite and MWNTs electrodes. The energy density of the hybrid capacitor can reach 32.91 W h/kg even at a current density of 10 mA/cm^2 in 1.0 M $LiClO_4$ electrolyte, which is comparable to that of a manganese oxide/activated carbon hybrid capacitor.

Keywords: Manganese oxide; Carbon nanotubes; Composite electrode; Supercapacitors

1. Introduction

As intermediate power and energy sources between conventional capacitors and batteries, supercapacitors or electrochemical capacitors (ECs) have achieved much attention in many fields, such as hybrid power sources, back-up power storage, peak power sources, and so on [1,2]. Based on the charge storage mechanism, there are two major categories [1,3,4]: (1) electric double-layer capacitors (EDLC) which store energy by utilizing the double-layer capacitance arising from the charge separation at the electrode–electrolyte interface, (2) pseudocapacitors which store energy by utilizing the pseudocapacitance arising from the fast and reversible Faradic reactions. To take full advantage of double-layer capacitance and pseudocapacitance, many metal oxide/carbon composite electrodes have been investigated for ECs [5–11]. Recently, hybrid capacitors using an EDLC–pseudocapacitor were introduced to increase the energy density and maintain the extended cycle life [6,12–14].

Carbon nanotubes (CNTs) are attractive materials for ECs because of their superb properties such as unique network of mesopores, high electrochemically accessible surface area of porous nanotubes arrays, excellent electronic conductivity and useful chemical stability [4,15–17]. Unfortunately, the relatively low capacitance and high cost preclude their practical applications. Presently, CNT composites have been used to overcome the disadvantages [4,7–9,17]. Manganese can be present in various valence states, and its oxides are promising candidates for ECs because of their low cost and being environmentally friendly [10–13,18,20,21]. Manganese oxide/activated carbon hybrid capacitor has been designed with aqueous electrolyte [12,13]. However, the narrow operating potential window limits the energy density besides the expensive current collector.

In this study, we employ M/M composite and MWNTs as EC electrodes with organic electrolyte that has a wide operating potential window. The electrochemical behaviors of the symmetric and asymmetric hybrid capacitors are contrasted at various current densities. It was found that the hybrid capacitor showed better performance.

---

* Corresponding author. Tel.: +86 28 85223721; fax: +86 28 85223978.
E-mail address: guixin68@yahoo.com (G.-X. Wang).

0167-2738/$ - see front matter © 2005 Elsevier B.V. All rights reserved.
doi:10.1016/j.ssi.2005.02.005

2. Experimental

2.1. Preparation of specimens

MWNTs were synthesized by pyrolysis of methane with NiO/La_2O_3 catalyst. They were refluxed with 3.0 M HNO_3 at 110 °C for 6.0 h, then cleaned with distilled water and dried under IR lamp. The purity is about 95 wt.%, and the diameters of the nanotubes are between 3 and 20 nm. The specific area of 476.10 m^2/g was obtained by nitrogen adsorption at 77 K.

Manganese oxide was prepared as follows: manganese acetate was blended with $KMnO_4$ and ethanol followed by being ground in an agate mortar. Then, the precursor was heated at 50–70 °C for nearly 10 h. Finally, the product was rinsed until the pH was near 7, and dried at 100–130 °C for 5–15 h. The specific area determined from BET measurement is 102.80 m^2/g.

2.2. Characterization

The products were characterized using transmission electron microscopy (TEM, JEOL JEM-100CX, Japan), scanning electron microscopy (SEM, JEOL JSM-5900LV, Japan), thermogravimetric analysis (TGA) and X-ray diffraction (XRD). TGA was performed from 40 to 700 °C at 10 °C/min ramp rate under a nitrogen atmosphere using a Perkin-Elmer TGA7 machine. XRD was recorded on a Philips X'Pert MPD diffractometer (Cu Kα radiation).

2.3. Electrode preparation and electrochemical characterization

Prepared manganese oxide was mixed with 25 wt.% of MWNTs by ultrasonic vibration in ethanol for 30 min, and then the resulted composite was thoroughly homogenized in an agate mortar with 5 wt.% PTFE binder to make a slurry to coat the cleaned aluminum current collector. The sheets were rolled to get an appropriate thickness of 100 μm. After drying at 100 °C under vacuum for 8.0 h, they were cut into 0.6 cm^2 wafers and used as electrodes. While, electrodes including MWNTs and PTFE binder (19:1 in mass) were also prepared. For comparison, a hybrid capacitor using M/M composite as positive electrode and MWNTs as negative electrode and two symmetric capacitors based on M/M composite electrodes and MWNTs electrodes, respectively, were assembled in an argon-filled glove box by sandwiching a microporous separator (Celgard 2400) between two electrodes. A 1.0 M $LiClO_4$/ethylene carbonate (EC)–diethyl carbonate (DEC) (1:1 in vol.) was used as electrolyte. In the hybrid capacitor, the active weight ration of the M/M composite positive electrode and the MWNTs negative electrode was 1:2.3, which was calculated using the 36.1 × 4 F/g specific capacitance for the M/M composite and 15.4 × 4 F/g specific capacitance for the MWNTs measured in the symmetric ECs at 10 mA/cm^2 current density. All devices were tested with constant current charge/discharge models at 298 K using a DC-5 battery-testing instrument (Shanghai Zhengfang Instruments).

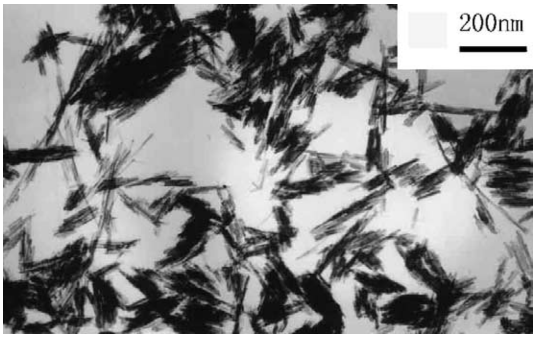

Fig. 1. TEM image of the manganese oxide.

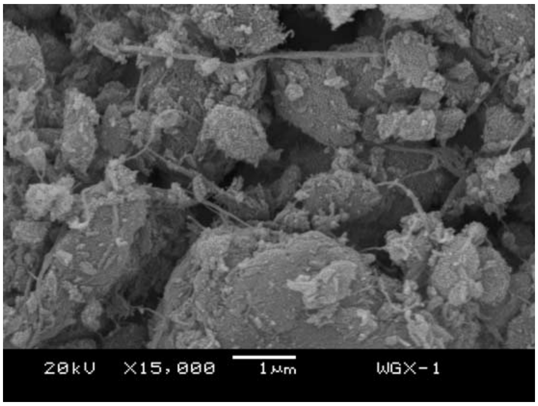

Fig. 2. SEM image of the M/M composite.

3. Results and discussion

TEM image (Fig. 1) reveals that the as-synthesized manganese oxide powder is made of needle-like particles. It is estimated that the nanocrystallites are about 100–300 nm in length and 20–40 nm in diameter. Nanostructures of manganese oxide are thought to be beneficial to ionic charge transport [19].

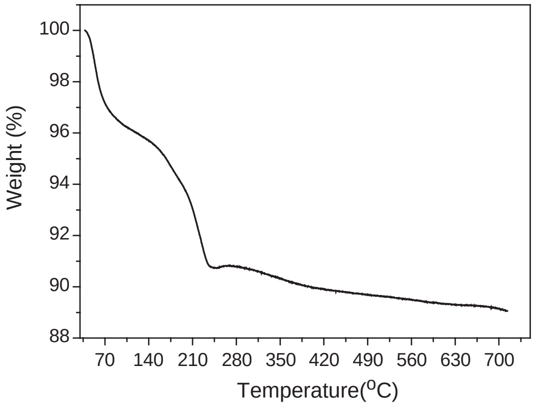

Fig. 3. TGA curve of the manganese oxide.

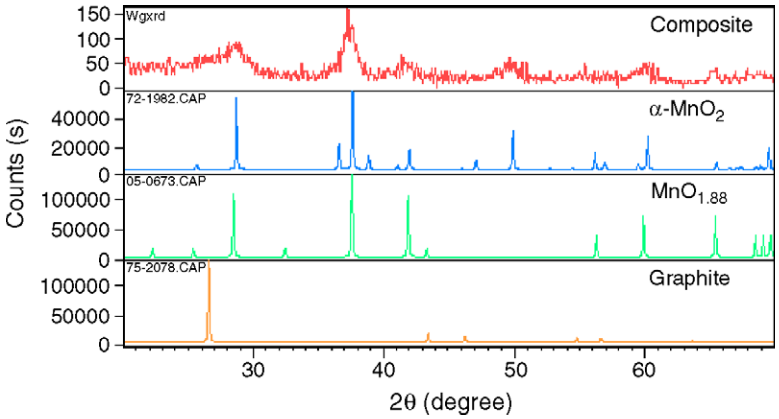

Fig. 4. XRD pattern of the M/M composite.

From the SEM image (Fig. 2) of the M/M composite, manganese oxide nanocrystallites agglomerate into spherical grains which are randomly contacted by entangled and cross-linked MWNTs in a quasi three-dimensional network. Each grain seems to result from the agglomeration of smaller particles, which is consonant with the TEM result.

Fig. 3 shows the TGA curve of the manganese oxide, the weight loss is rather fast up to 250 °C due to evaporation of physically adsorbed water, then up to 450 °C, the removal of water from the interlayer, and then it slows down (in agreement with the report [20]).

In the XRD pattern of the M/M composite (Fig. 4), that no discernible peak is detected confirms the disordered structure of the composite. Broad peaks related to a poorly crystallized compound may originate from the small particle size and amorphous nature of the powder. From the XRD analysis, manganese oxide is composed of α-MnO_2 and $MnO_{1.88}$.

Fig. 5 exhibits a representative plot of galvanostatic discharge capacity of the three types of ECs. The almost linear curve indicates a constant discharge capacitance, but perfect linear curves were not obtained compared with the case of EDLC. This may be due to the nonlinear redox process occurring at the electrode during discharging [6]. Capacities (mA h/g) can be converted to capacitances (F/g) by the following formula 1

$$\frac{\mathrm{F}}{\mathrm{g}} = i(\mathrm{A})\cdot\frac{dt(\mathrm{s})}{dV(\mathrm{V})}\cdot\frac{1}{\mathrm{g}} = \frac{\mathrm{mAh}}{\mathrm{g}}\cdot\frac{1000}{dV(\mathrm{V})\cdot 3600} = \frac{1}{3.6\cdot dV(\mathrm{V})}\cdot\frac{\mathrm{mAh}}{\mathrm{g}} \quad (1)$$

The relation is only valid if the voltage is linear with time, nonFaradaic function [22]. The capacitances in this paper were all obtained by calculating using the expression within linear discharge voltage range. From the discharge curves, we can also know that the hybrid capacitor has a wider discharge voltage though all of them were tested under the same conditions, which resembles the manganese oxide/ activated carbon hybrid capacitor [12,13].

Fig. 6 shows the maximum specific capacitance as a function of discharge current density for the three kinds of ECs. For the hybrid capacitor, the maximum specific capacitance of 56 F/g was obtained. The value is respectively 1.3 times that obtained from the M/M composite-based EC and 3.4 times that obtained from the MWNTs-based EC. Similar to the $Ni(OH)_2$/activated carbon composite hybrid capacitor [6].Though the specific capacitance was enhanced

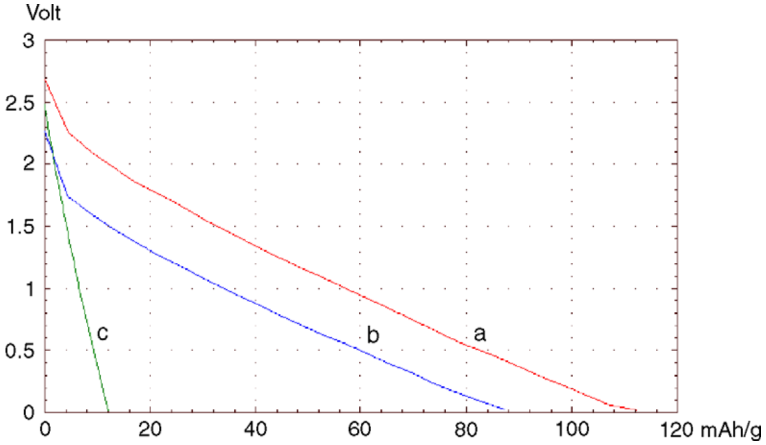

Fig. 5. Galvanostatic discharge curves of (a) hybrid capacitor, (b) M/M composite-based EC, (c) MWNTs-based EC.

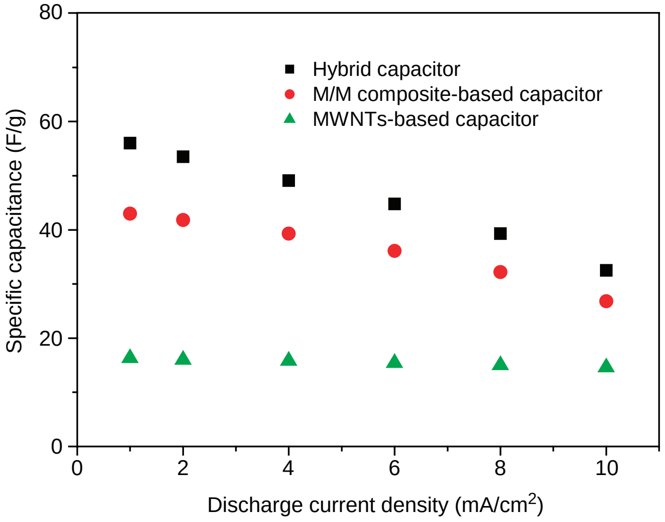

Fig. 6. Specific capacitance of the three kinds of ECs as a function of current density.

greatly, the hybrid capacitor showed relatively poor power characteristics in contrast with the symmetric ones, which was also confirmed in Fig. 7. Normalized capacitance was obtained from Eq. (2):

$$\text{Normalized capacitance} = \frac{C}{C\left(1\ \text{mA/cm}^2\right)} \tag{2}$$

where C is specific capacitance (F/g) of a capacitor. The symmetric ECs showed better power characteristics between 1 and 10 mA/cm^2 current density, especially MWNTs-based EC. These attribute to the different charge storage mechanisms. The MWNTs-based EC stores energy mainly by EDLC because of the perfect linear discharge curve, while the M/M composite-based EC stores energy mainly by pseudocapacitance because of the quasi-linear discharge curve. The asymmetric hybrid capacitor combines the advantages of non-Faradic and Faradic charge elements [22,23]. Therefore, we can postulate that in the hybrid capacitor, the MWNTs negative electrode stores charge electrostatically across the double-layer interphase at the interface by cation adsorption, while the M/M composite positive electrode stores charge indirectly in a chemical way involving Li$^+$ insertion/desertion. The evidence is under investigation.

Energy density (E) was obtained from Eq. (3)

$$E = \frac{1}{2}CV^2 \tag{3}$$

where V is discharge voltage (V). The energy densities that take into account only the weight of the active electrode materials are reported in Fig. 8. Even at a current density of 10 mA/cm^2, the hybrid capacitor still has a higher energy density compared with the symmetric ones. This comes from the combination of higher capacitance and expanded voltage.

From the curves in Fig. 9, the hybrid capacitor has higher capacitances and less capacitance fading. For the electro-

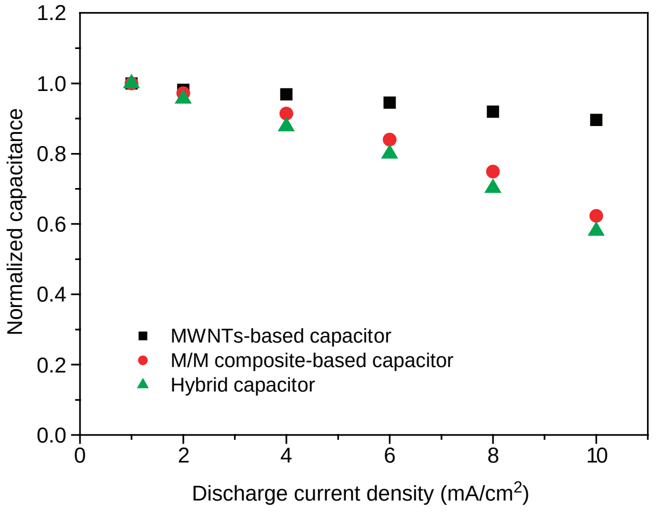

Fig. 7. Comparison of capacitance fading of the three kinds of ECs at various current densities.

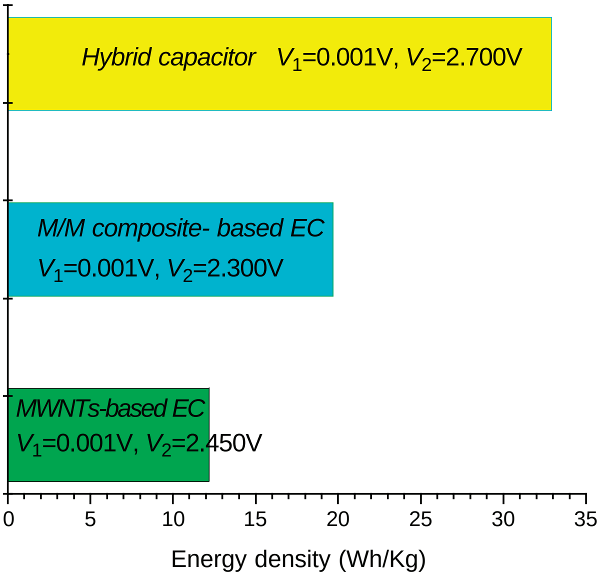

Fig. 8. Characteristics of energy density of the three kinds of ECs at 10 mA/ cm^2 current density.

chemical performance of MWNTs has been greatly improved by M/M composite, we think that the single MWNTs are mainly affected by the impurities along with the particles aggregation. When mixed with manganese oxide, MWNTs generate electron conduction channels inside the electrode layer by making contacts among manganese oxide particles and contribute to the electrolyte reservoir and the charge storage by their unique morphology. The effect of impurities can be negated because of the low content of MWNTs. Therefore, the pseudocapacitance faradic reaction is enlarged enough to show ideal capacitor behavior. At the same time, MWNTs will also contribute to the charge storage by the EDLC mechanism. Additionally, the cylindrical structure of CNT may contribute to the increase of the filling factor which is related to the discharge capacitance [17] and the linear structure for CNT might contribute to the rapid Li^+ insertion and removal [24]. For the manganese oxide, the valence state of Mn may change from 0 to IV over a wide potential range [18], which is easier for the metastable $MnO_{1.88}$ to transfer electrons because the valence state is between +3 and +4. Also, α-MnO_2 has excellent electrochemical activity [21]. The intercalation of lithium ions into MnO_2 structure causing redox transitions benefits the pseudocapacitance faradic reaction [20,25]. After many cycles, capacitance fading may originate from the slow dissolution of Mn due to the disproportionation of Mn^{3+} into Mn^{4+} and soluble Mn^{2+} [26].

Recently, $Ni(OH)_2$/activated carbon [6] and manganese oxide/activated carbon hybrid capacitors [12,13] have been designed to improve the energy densities, respectively. In this study, the hybrid capacitor improved the capacitance and energy density. The overall capacitance C_T of a capacitor is contributed by both positive (C_p) and negative (C_n) electrodes and can be calculated using Eq. (4):

$$\frac{1}{C_T} = \frac{1}{C_p} + \frac{1}{C_n} \tag{4}$$

where C_p and C_n are equal in a symmetric capacitor and unequal in an asymmetric one [23]. Consequently, in a pseudocapacitor/EDLC hybrid capacitor, the C_T is close to the double-layer capacitance C_d, not the 1/4 C_d (C_T of symmetric capacitor) on a mass basis because the pseudocapacitance is higher than $C_{d.}$ Thus, the charge capacitance of the double-layer component electrode can be fully utilized, and the capacitance for the hybrid capacitor can be increased. At 10.0 mA/cm^2 current density, the hybrid capacitor was cycled 300 cycles with a 27.72% decrease of the maximum capacitance, which is significantly smaller than those based on both M/M composite electrodes (42.21%) and MWNTs electrodes (52.47%). Certainly, further work to improve the cycling stability and power density is necessary.

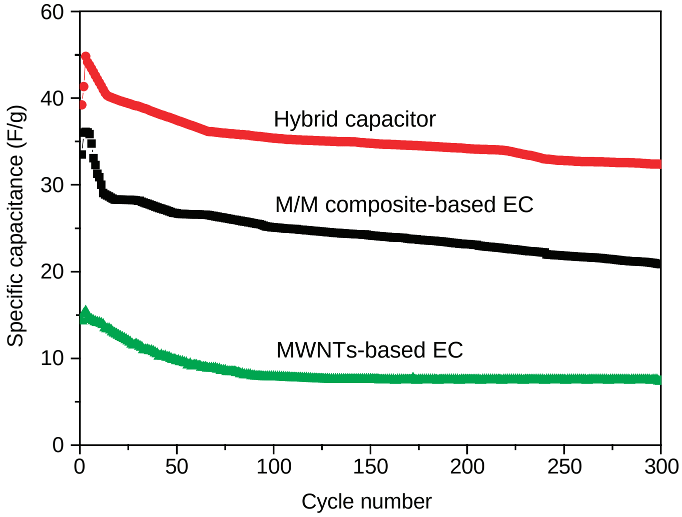

Fig. 9. Cycle performance of the three kinds of ECs at $10mA/cm^2$ current density.

4. Conclusions

In summary, M/M composite electrodes have been considered to improve the electrochemical properties of the single MWNTs electrodes, and a hybrid capacitor working in organic electrolyte has been presented. By using M/M composite as positive electrode and MWNTs as negative electrode, the hybrid capacitor shows good capacitance and energy characteristics despite its poor power characteristics. Even at a current density of 10 mA/cm^2, the energy density of the hybrid capacitor can reach 32.91 W h/kg, which is comparable to that of a manganese oxide/activated carbon hybrid capacitor. It is anticipated that the application of the low cost and environmentally friendly manganese oxide to modify carbon nanotubes can significantly increase the performance of carbon nanotubes in ECs. What is more, the concept of hybrid capacitor will be an interesting alternative to improve the performance of current ECs.

Acknowledgements

This work was supported by financial support from the Knowledge Innovation Program of the Chinese Academy of Sciences (KJCX1-06-04) and Ningbo Shanshan Science and Technology Zone LTD.

References

[1] B.E. Conway, Electrochemical Supercapacitors: Scientific Fundamentals and Technological Applications, Kluwer Academic/Plenum, 1999.
[2] R. Kötz, M. Carlen, Electrochim. Acta 45 (2000) 2483.
[3] S. Sarangapani, B.V. Tilak, C.P. Chen, J. Electrochem. Soc. 143 (1996) 3791.
[4] E. Frackowiak, F. Béguin, Carbon 39 (2001) 937.
[5] T. Kudo, Y. Ikeda, T. Watanabe, M. Hibino, N. Miyayama, H. Abe, K. Kajita, Solid State Ion. 152–153 (2002) 833.
[6] J.H. Park, O.O. Park, K.H. Shin, C.S. Jin, J.H. Kim, Electrochem. Solid-State Lett. 5 (2002) H7.
[7] R.Z. Ma, B.Q. Wei, C.L. Xu, J. Liang, D.H. Wu, Bull. Chem. Soc. Jpn. 73 (2000) 1813.
[8] G. Arabale, D. Wagh, M. Kulkarni, I.S. Mulla, S.P. Vernekar, K. Vijayamohanan, A.M. Rao, Chem. Phys. Lett. 376 (2003) 207.
[9] X. Qin, S. Durbach, G.T. Wu, Carbon 42 (2004) 451.
[10] H.Y. Lee, S.W. Kim, H.Y. Lee, Electrochem. Solid-State Lett. 4 (2001) A19.
[11] J.K. Chang, C.T. Lin, W.T. Tsai, Electrochem. Commun. 6 (2004) 666.
[12] T. Brousse, M. Toupin, D. Bélanger, J. Electrochem. Soc. 151 (2004) A614.
[13] M.S Hong, S.H. Lee, S.W. Kim, Electrochem. Solid-State Lett. 5 (10) (2002) A227.
[14] J.P. Zheng, J. Electrochem. Soc. 150 (2003) A484.
[15] C.M. Niu, E.K. Sichel, R. Hoch, D. Moy, H. Tennent, Appl. Phys. Lett. 70 (1997) 1480.
[16] H.B. Ray, A.Z. Anvar, A. de H. Walt, Science 297 (2002) 787.
[17] K. Honda, M. Yoshimura, K. Kawakita, A. Fujishima, Y. Sakamoto, K. Yasui, N. Nishio, H. Masuda, J. Electrochem. Soc. 151 (2004) A532.
[18] J.H. Jiang, A. Kucernak, Electrochim. Acta 47 (2002) 2381.
[19] M.Q. Wu, G.A. Snook, G.Z. Chen, D.J. Fray, Electrochem. Commun. 6 (2004) 499.
[20] R.N. Reddy, R.G. Reddy, J. Power Sources 124 (2003) 330.
[21] M. Toupin, T. Brousse, D. Bélanger, Chem. Mater. 14 (2002) 3946.
[22] G.G. Amatucci, F. Badway, A.D. Pasquier, T. Zheng, J. Electrochem. Soc. 148 (2001) A930.
[23] W.G. Pell, B.E. Conway, J. Power Sources 136 (2004) 334.
[24] K. Tanaka, Carbon Nanotube, Chap. 3, NTS Inc., Tokyo, 2001.
[25] J.W. Long, A.L. Young, D.R. Rolison, J. Electrochem. Soc. 150 (2003) A1161.
[26] R.J. Gummow, A. de Kock, M.M. Thackery, Solid State Ion. 69 (1994) 59.